SUPPLEMENTAL MATERIAL

Constitutively-active TRPC channels of adipocytes confer a mechanism for sensing dietary fatty acids and regulating adiponectin

Piruthivi Sukumar[1,2], Alicia Sedo[1,2], Jing Li[1,2], Lesley A Wilson[1,2], David O'Regan[1,4], Jonathan D Lippiat[2], Karen E Porter[1,3], Mark T Kearney[1,3], Justin FX Ainscough[1,3] & *David J Beech[1,2,3]

[1]Multidisciplinary Cardiovascular Research Centre, [2]Faculty of Biological Sciences, and [3]Faculty of Medicine & Health, University of Leeds, Leeds, LS2 9JT, UK.
[4]Department of Cardiac Surgery, Leeds General Infirmary, Great George Street, Leeds, LS1 3EX, UK.

*Author for correspondence: Prof David J Beech, Faculty of Biological Sciences, Garstang Building, Mount Preston Street, University of Leeds, Leeds, LS2 9JT, UK; d.j.beech@leeds.ac.uk; Tel +44 (0) 113 34 34323; Fax +44 (0) 113 34 34228.

Supplemental Methods

Human and mouse tissues

Left internal mammary artery segments with fat were obtained anonymously and with informed consent from patients undergoing open heart surgery. Approval was granted by the Local Research Ethics Committee. Eight week old male C57BL/6 mice were killed by CO_2 asphyxiation and cervical dissociation in accordance with Schedule 1 Code of Practice, UK Animals Scientific Procedures Act 1986. Thoracic aorta with fat and epididymal fat were placed in ice-cold Hanks solution.

Electrophysiology

Whole cell patch-clamp recordings were performed at room temperature[1]. Patch pipette solution 1 contained (mmole/L): 135 CsCl, 2 $MgCl_2$, 5 Na_2ATP, 0.1 NaGTP, 1 EGTA and 10 HEPES at pH 7.2 (CsOH). Patch pipette solution 2 contained (mmole/L): 115 CsCl, 2 $MgCl_2$, 5 Na_2ATP, 0.1 NaGTP, 10 EGTA, 5.7 $CaCl_2$ and 10 HEPES at pH 7.2 (CsOH). Pipette solution 1 was for 3T3-L1 cell recordings. Pipette solution 2 was for HEK 293 cell studies. The extracellular solution was SBS or SBS in which Ca^{2+} was substituted by Ba^{2+} where indicated. Whole cell patch-clamp signals were amplified with an Axopatch 200B patch clamp amplifier (Molecular Devices, USA) and software was Signal 3.05 (CED, UK). A ramp voltage protocol from -100 mV to +100 mV of 1 s duration was applied every 10 s from a holding potential of 0 mV. Current signals were filtered at 1 kHz and digitally sampled at 3 kHz. Patch pipettes had resistances of 3-5 MΩ.

Immunostaining

Cells were fixed with 3 % formaldehyde and then incubated with primary antibodies in 0.5 % donkey serum overnight at 4 °C and then with FITC-conjugated secondary antibodies for 2 hr at room temperature. Coverslips were mounted using DAPI-hardest mounting medium (Vector Labs). Perivascular and epididymal fat tissue and aortic segments were fixed in 10 % formalin and embedded in paraffin. 8 μm sections were cut, hot-plated and dried overnight. Dewaxing, rehydration, and antibody

staining were according to standard protocols. Sections were incubated with primary antibodies overnight at 4 ºC, labelled using ABC kit and visualised with 3,3'-diaminobenzidine substrate (Vector labs). Sections were counter-stained with eosin.

Western blotting

Cells or minced tissue were lysed with 1.25 % SDS containing 1 mmole/L dithiothreitol at 80-100 °C for 15 min. Proteins were separated on 10 % SDS-PAGE gels and transferred to nitrocellulose membrane (Millipore) and probed with primary antibodies diluted in 5 % milk. Secondary antibody was conjugated with horseradish peroxidase. Incubation in primary antibody was overnight at 4 °C and in secondary antibody was 2 hr at room temperature. Membranes were washed with PBST and labelling was detected with ECLplus chemiluminescence reagent (Amersham). Antibodies were: anti-PPARγ (1:100; Santa Cruz), anti-β actin (1:1000; Santa Cruz), anti-TRPC1 (1:500; custom made T1E3) or anti-TRPC5 (1:100; custom made T5E3).

RNA isolation, RT-PCR and microfluidic cards

Total RNA was isolated using a standard TriReagent protocol and treated with DNAse I (Ambion); an aliquot was used for cDNA synthesis using a high capacity RT kit (Applied Biosystems, UK) containing Oligo-dT and random primers. PCR primer sequences are in Online Table II. Primers were used at 0.5 μmole/L with 3 mmole/L Mg^{2+}. Thermal cycling was 40 cycles of: 94 °C (30 s); 56.6 °C (1 min); 72 °C (1 min). PCR products were electrophoresed on 1.5 % agarose gels containing ethidium bromide. Direct sequencing confirmed product identity. Custom TaqMan Array (MFC_384) microfluidic cards were loaded with primers and Taqman probes (Applied Biosystems) and real-time PCR was performed in an ABI prism 7900HT Sequence Detection System controlled by SDS 2.2 software (Applied Biosystems).

DNTRPC5 (DNT5) specificity

cDNA encoding DNT5 was transfected into wild-type HEK 293 cells or HEK 293 cells stably over-expressing TRPM2 or TRPM3 channels. Transfection was achieved using FuGene HD transfection reagent (Roche) according to the manufacturer's protocol. Briefly, transfection reagent and 2 μg of plasmid DNA was added to 194 μl of Opti-MEM medium (Gibco) and the mixture was incubated at room temperature for 15-20 min and then added to 80 % confluent cells in 10 cm^2 plate (one well of a 6-well plate) containing 2 ml of culture medium. TRPM2 and TRPM3 were investigated by measuring intracellular Ca^{2+}, as described for TRPC5 recordings. For voltage-dependent K^+ current recordings, 500 ms duration voltage steps were applied starting from -120 mV and incrementing by 10 mV every 10 s to a final voltage of +80 mV. The holding potential was -80 mV.

Supplemental Results

More detailed information for the adiponectin measurements in fat-fed mice is as follows: Statistical comparison of the groups using an unpaired *t*-test not assuming equal variances gave a *P* value of 0.001, indicating a high probability that our conclusion is correct (i.e. that DNT5 stimulated the generation of adiponectin). Independent analysis of each set of data arising from different litters also indicated statistically significant differences between the test and control groups (data not shown). 15 male mice from 2 litters were investigated in the chow group, and 24 male mice from 3 litters in the fat-fed group.

Supplemental Discussion

There is a report of TRPC1, TRPC4 and TRPC6 mRNAs in human pre-adipocytes[2]. These data support our undifferentiated mouse 3T3-L1 data, which suggest that TRPC1 mRNA is detectable in pre-adipocytes. We did not detect TRPC4 or TRPC6 mRNA in the 3T3-L1 cells. The study of human pre-adipocytes did not provide quantitative data or make a comparison with differentiated (mature) adipocytes.

Supplemental Figure Legends

Online Figure I. DNTRPC5 (DNT5) specificity, transgene construct and detection.
A, Diagram of the membrane topology of a single TRPC5 protein, showing the location of the LFW amino acid sequence that was mutated to AAA in order to generate a dominant negative (DN) TRPC5 (DNT5) that inhibits Ca^{2+} flux. **B**, Mean normalised data showing the effects of transfection of HEK 293 cells with vector expressing DNT5 (DNTRPC5) or vector alone (controls). Four sets of experiments are shown for cells: (i) with stable conditional over-expression of wild type TRPC5; (ii) with stable conditional over-expression of wild type TRPM2; (iii) with stable conditional over-expression of wild type TRPM3; or (iv) not transfected but showing endogenous voltage-gated K^+-current (K_V current). TRPM2 was activated by 1 mmole/L H_2O_2 and TRPM3 by 10 μmole/L pregnenolone sulphate. Each experimental set had its own control even though only one control bar is shown. The data show that DNT5 inhibited wild type TRPC5 but not TRPM2, TRPM3 or K_V current. **C**, Diagram of the DNT5 transgene construct containing LacZ and DNT5 either side of a bi-directional promotor complex with a tetracycline response element (TRE), two opposing minimal CMV promoters (CMV_{min}), and SV40 and β-globin polyadenylation sequences. Ase1 sites were used for construct linearization and removal of plasmid sequence prior to injection. **D**, Validation of DNT5-specific PCR primers (see Online Table II for sequences) in PCR reactions that used wild-type (WT) TRPC5 or DNT5 cDNAs as templates. DNT5 primers only generated a product (360 bp) in reactions containing DNT5 template. WT primers generated products from both templates as they recognise sequence outside the mutated site of DNT5. 'M' indicates the DNA marker ladder.

Online Figure II. Confirmation of differentiation in mouse 3T3-L1 cells.
A, Oil-Red-O staining of undifferentiated (**a**) and differentiated (**b**, **c**) 3T3-L1 cells (scale bar, 100 μm). **B**, Mean abundances of PPARγ and aP2 mRNAs in undifferentiated (Undiff) and differentiated (Diff, adipocytes) 3T3-L1 cells (n=3). **C**, Western blots for lysates from Undiff and Diff 3T3-L1, showing labelling by anti-PPARγ (top panel) and anti-β-actin (bottom panel) antibodies. Predicted masses of PPARγ and β-actin are 58 and 43 kDa. **D**, PCR products from total RNA with (+) and without (-) reverse transcriptase (RT) reactions. Expected PCR product sizes were 363 bp (adiponectin) and 191 bp (leptin). **E**, Loading controls for the western blots in Figure 1C showing single bands labelled by anti-β-actin antibody.

Online Figure III. Messenger RNA species encoding additional TRP channels.
PCR products from total RNA of mouse brain or differentiated (Diff) or undifferentiated (Undiff) 3T3-L1 cells with (+) or without (-) reverse transcriptase

(RT) reaction. Expected PCR product sizes were 222 bp (TRPC3), 349 bp (TRPC4), 272 bp (TRPC6), 193 bp (TRPC7), 232 bp (TRPV4), 186 bp (TRPP2). TRPC3, TRPC4, TRPC6 and TRPC7 mRNA species were detected in brain but not 3T3-L1 cells. TRPV4 and TRPP2 mRNA species were detected similarly in differentiated and undifferentiated 3T3-L1 cells. TRPC2 mRNA was detected on the microfluidic card and was indicated to be slightly up-regulated on adipocyte maturation (-1.4 PCR cycle shift). Although TRPC2 may be functionally relevant in murine adipocytes it was not studied further because it is not relevant to humans, where *TRPC2* is a pseudogene.

Online Figure IV. Control data for the detection of TRPC1 and TRPC5 proteins in 3T3-L1 cells by immunofluorescence.
Shown is labelling of undifferentiated (Undiff) and differentiated (Diff) 3T3-L1 cells with T1E3 anti-TRPC1 (**A**) or T5E3 anti-TRPC5 (**B**) antibodies. The controls were antibodies preadsorbed to their antigenic peptides (+pep). Positive labelling is indicated by the green colour of the FITC-conjugated secondary antibody. Cell nuclei were stained with DAPI (blue). Images are representative of 3 independent experiments. The scale bar is 20 μm and applies to all images.

Online Figure V. Immunofluorescence data for expression of TRPC1 and TRPC5 in mouse peri-vascular fat.
Immunostaining of mouse thoracic aorta (**a**) and the surrounding perivascular fat (**pvf**). Upper panels show positive staining (brown colour) for anti-TRPC1 (T1E3) and anti-TRPC5 (T5E3) antibodies, whereas lower panels show control experiments when antibodies had been boiled to denature the protein content (scale bar, 100 μm).

Online Figure VI. Validation of TRPC1 and TRPC5 knock-down by RNA interference in 3T3-L1 cells.
Mean quantitative real-time RT-PCR data for TRPC1, TRPC5 and TRPP2 mRNAs, showing specific knock-down of TRPC1 and TRPC5 mRNAs by the mixture of siRNAs targeting TRPC1 and TRPC5 (n=3). Each knock-down reaction was normalised to its own control from cells treated with scrambled siRNA.

Online Figure VII. Validation that fat-feeding induced inflammation.
Mean quantitative real-time RT-PCR data for interleukin-6 (IL-6) and tumour necrosis factor α (TNFα) mRNAs from adipose tissue of the mice fed chow (n=7) or high fat (n=7). The mice were from the groups used for analysis of adiponectin, as shown in the main paper. The data from fat-fed mice are normalised to those of the chow-fed mice.

Online Figure VIII. Suppression of mouse adipocyte Ca^{2+} entry by α-linolenic acid. Example confocal fluo-4 Ca^{2+} measurement from all adipocytes within a single field in a dish (control chow-fed mouse). Representative of n=5. Substances bath-applied to the cell were 100 μmole/L rosiglitazone (ros) and 50 μmole/L α-linolenic acid (lino.).

Online Figure IX. Diagram summarising the findings of the study. The grey square symbolises a mature adipocyte and the heterotetrameric cylinders at the top are TRPC 1 and 5 proteins around a central ion pore that is permeable to Ca^{2+} and Na^{+}. The large black cross on the horizontal white arrow indicates that the Ca^{2+} entry suppressed the generation of adiponectin. Adiponectin is anti-inflammatory and so

inhibition of adiponectin is described as leading to inflammatory effects that include atherosclerosis. Constitutive channel activity and enhancers of the TRPC1/5 channels are shown in the top left corner (e.g. stress factors). At the top right corner are examples of dietary factors that suppress the TRPC1/5 channel activity (e.g. ω-3 fatty acids). By inhibiting the channel, these factors reduce Ca^{2+} entry, reducing the inhibitory effect of the TRPC1/5-mediated Ca^{2+} entry on adiponectin; that is, the factors inhibit an inhibitor, conferring a double-negative that leads to a positive effect on adiponectin.

Supplemental Table Legends

Online Table I. Sequences of TRPC1 and TRPC5 siRNAs.

Online Table II. PCR primers.

Online Table III. Summary data for fatty acids that inhibited Gd^{3+}-evoked TRPC5 activity in HEK 293 cells. Fatty acids were tested at 50 μmole/L. The number of independent experiments (n) was 3 for each fatty acid.

Online Table IV. Negative results from screening of the fatty acid library against Gd^{3+}-evoked TRPC5 activity in HEK 293 cells. Fatty acids were tested at 50 μmole/L. The fatty acids which gave non-specific Ca^{2+} signals in non induced HEK 293 cells were omitted from final analysis. The number of independent experiments (n) was 3 for each fatty acid.

Supplemental References

1. Xu SZ, Sukumar P, Zeng F, Li J, Jairaman A, English A, Naylor J, Ciurtin C, Majeed Y, Milligan CJ, Bahnasi YM, Al-Shawaf E, Porter KE, Jiang LH, Emery P, Sivaprasadarao A, Beech DJ. TRPC channel activation by extracellular thioredoxin. *Nature*. 2008;451:69-72
2. Hu R, He ML, Hu H, Yuan BX, Zang WJ, Lau CP, Tse HF, Li GR. Characterization of calcium signaling pathways in human preadipocytes. *Journal of cellular physiology*. 2009;220:765-770

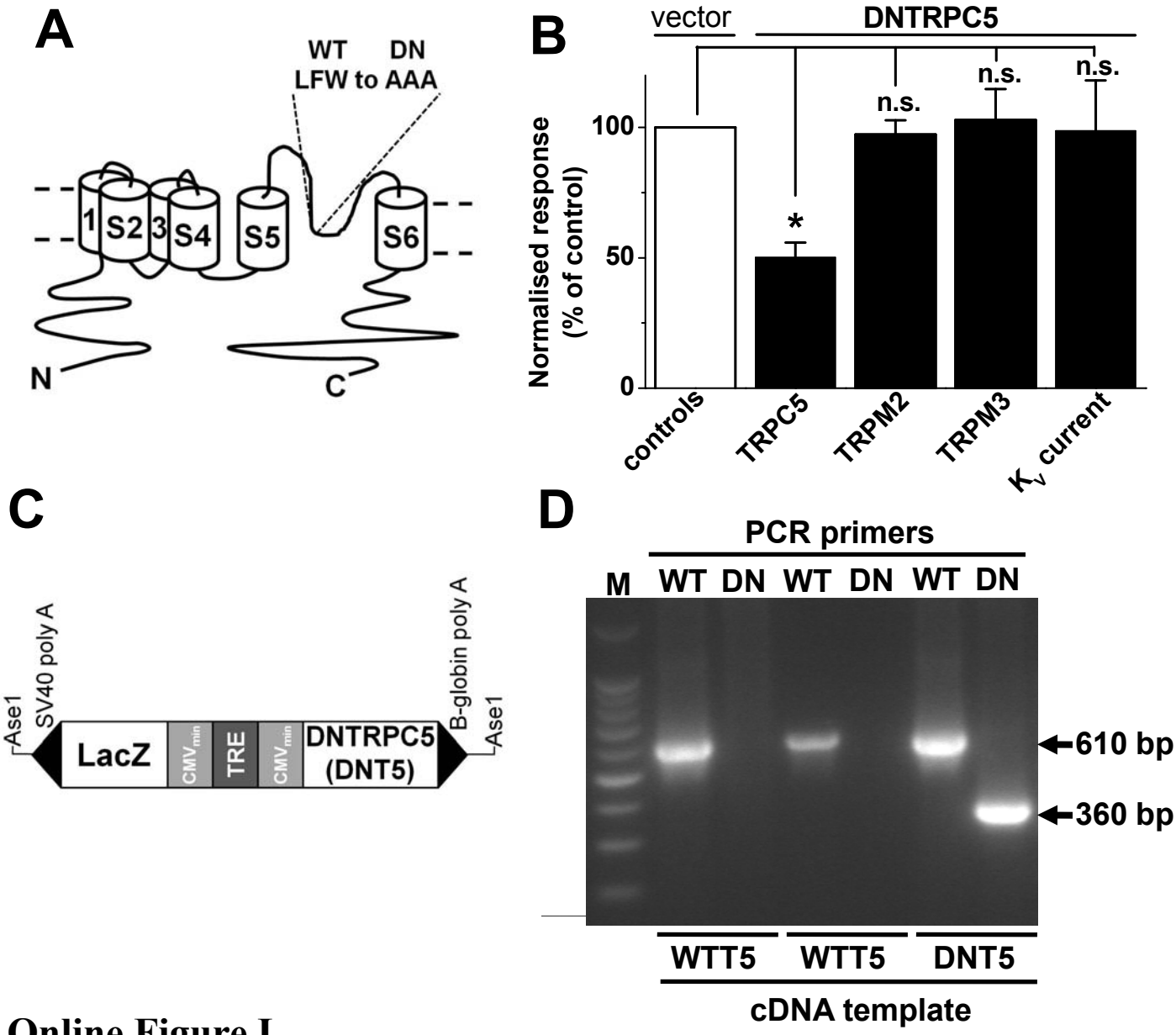

Online Figure I

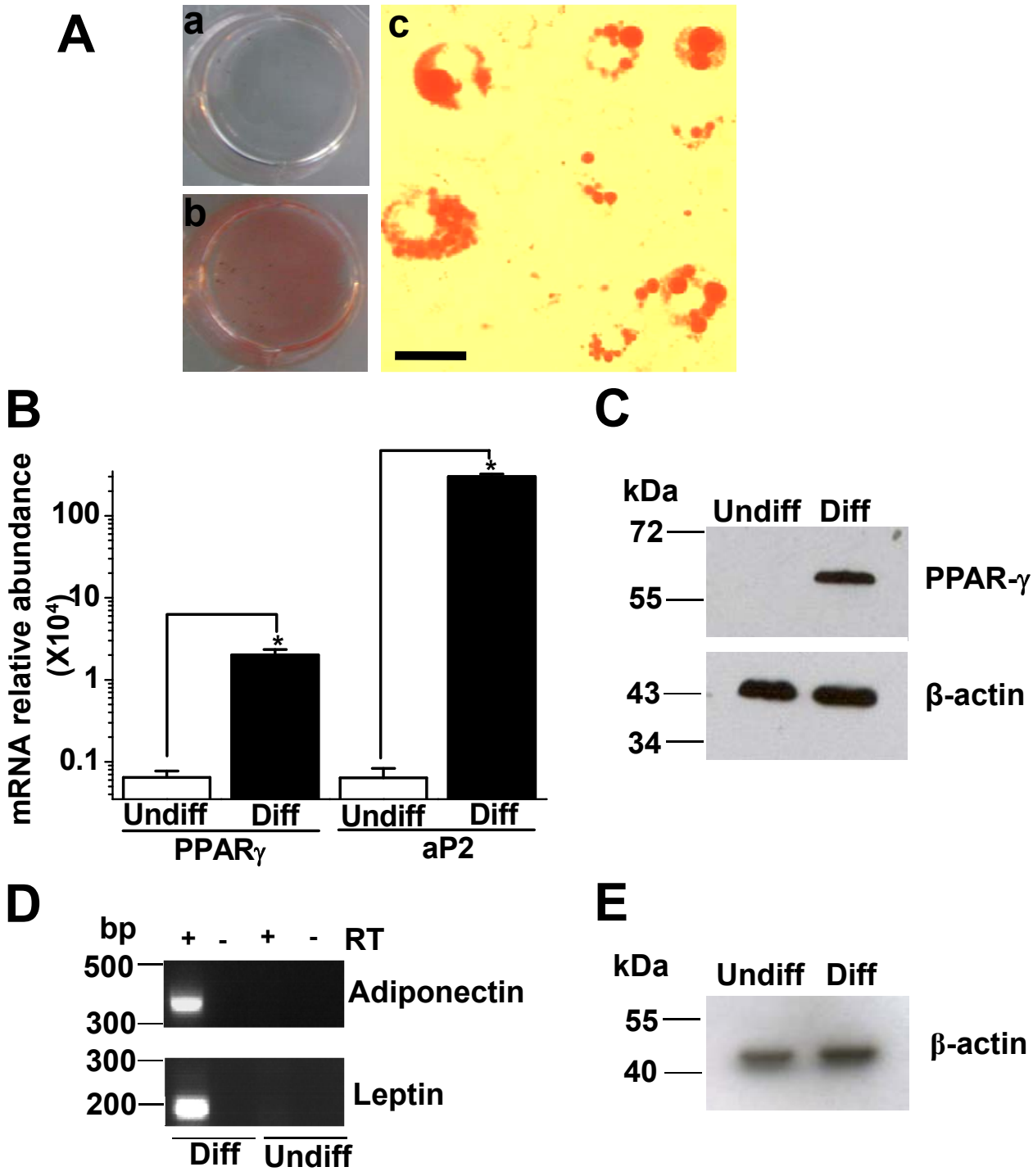

Online Figure II

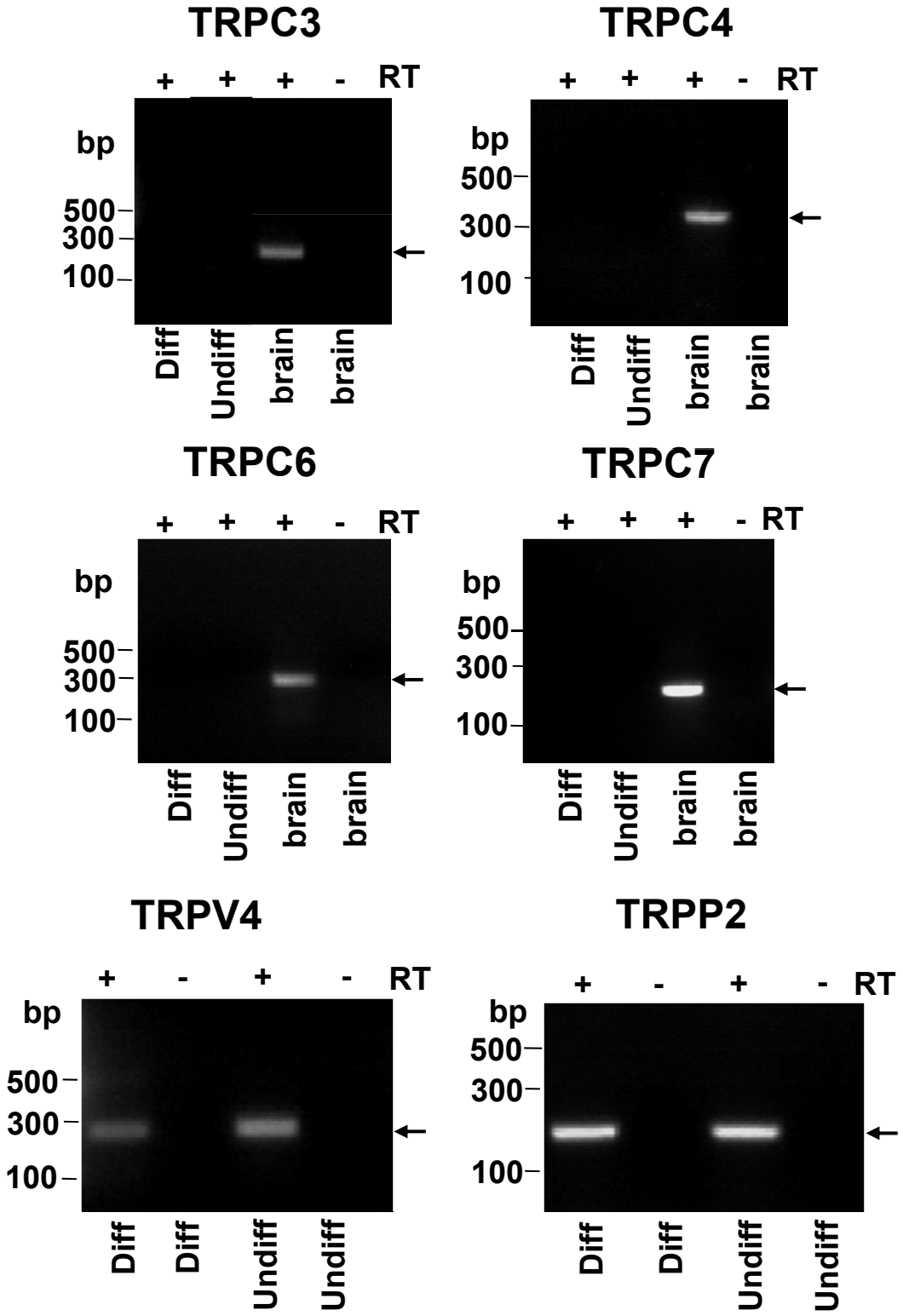

Online Figure III

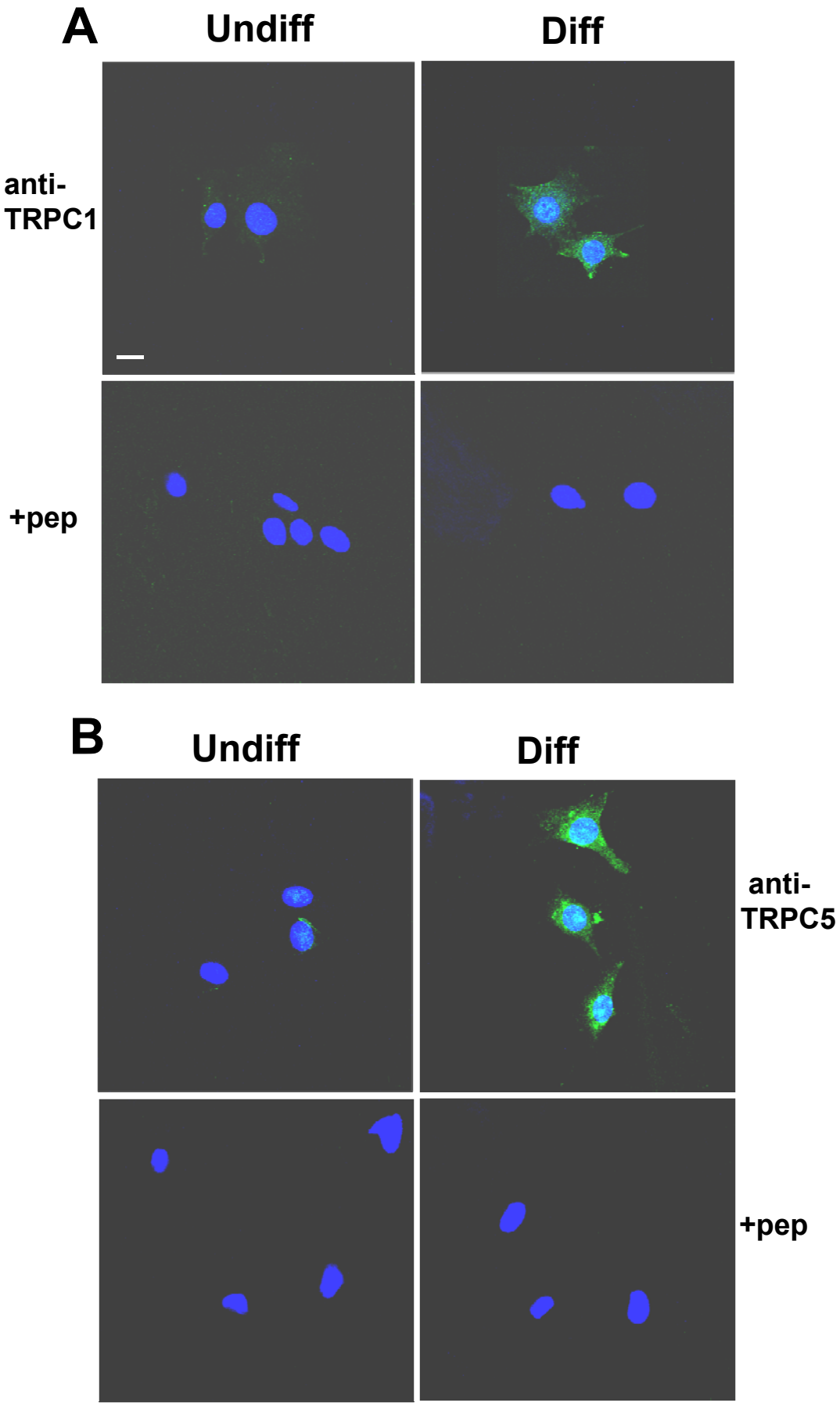

Online Figure IV

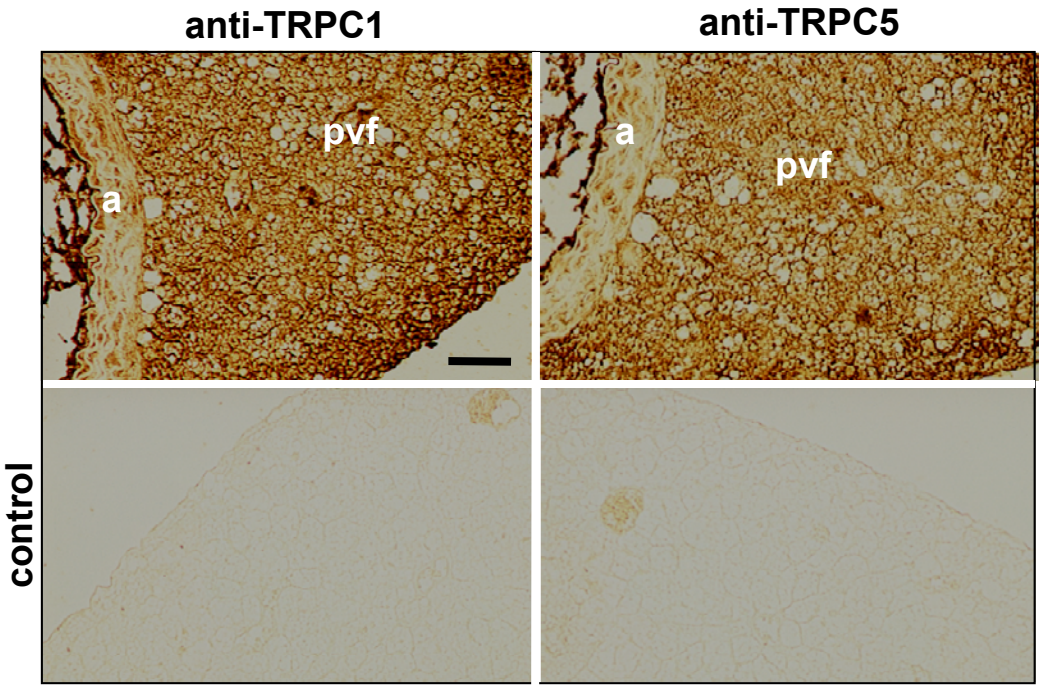

Online Figure V

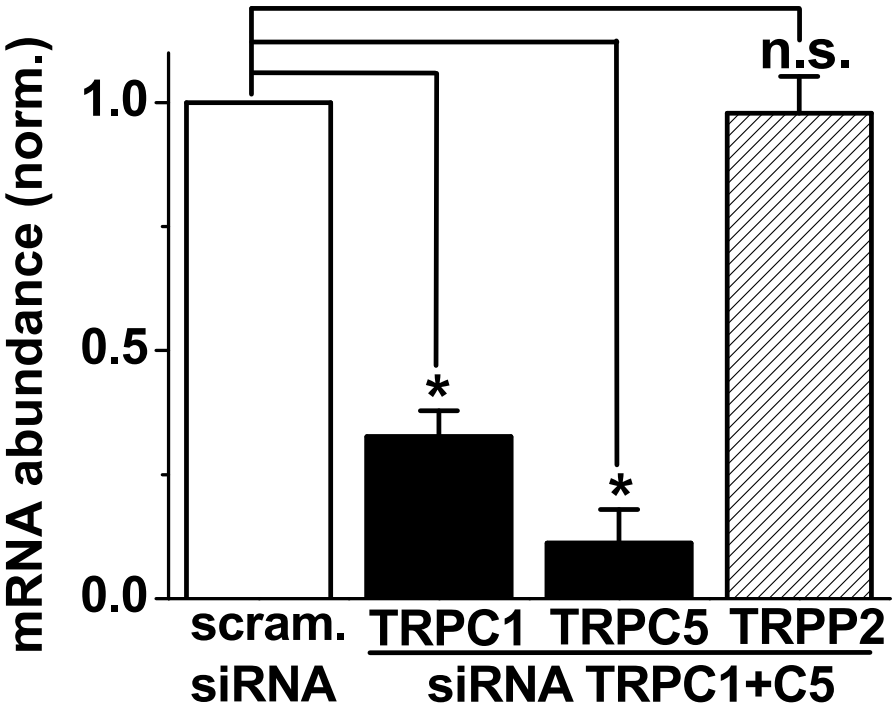

Online Figure VI

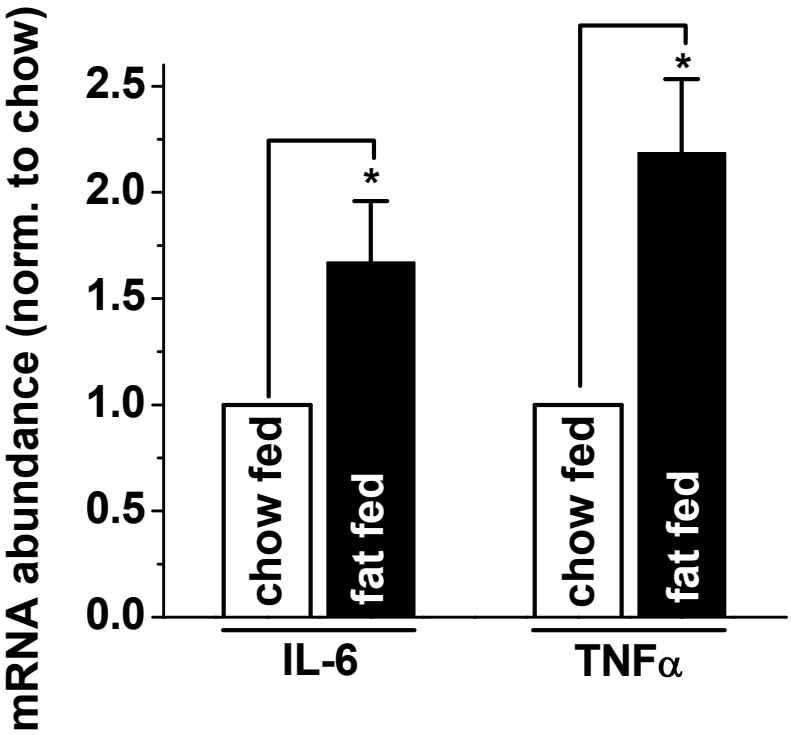

Online Figure VII

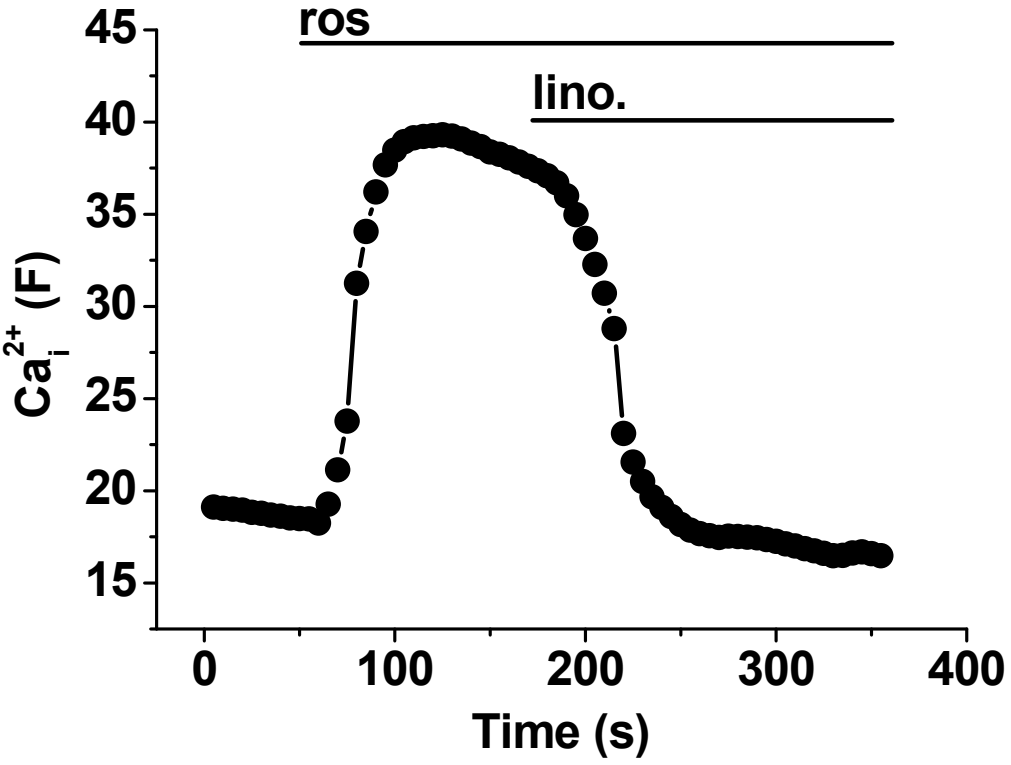

Online Figure VIII

•**constitutive activity**
•**stimulation by stress factors** (e.g. oxidized phospholipids)

•**inhibition by protective dietary chemicals**
ω-3 fatty acids (e.g. α-linolenic acid)
stilbenes (e.g. resveratrol)

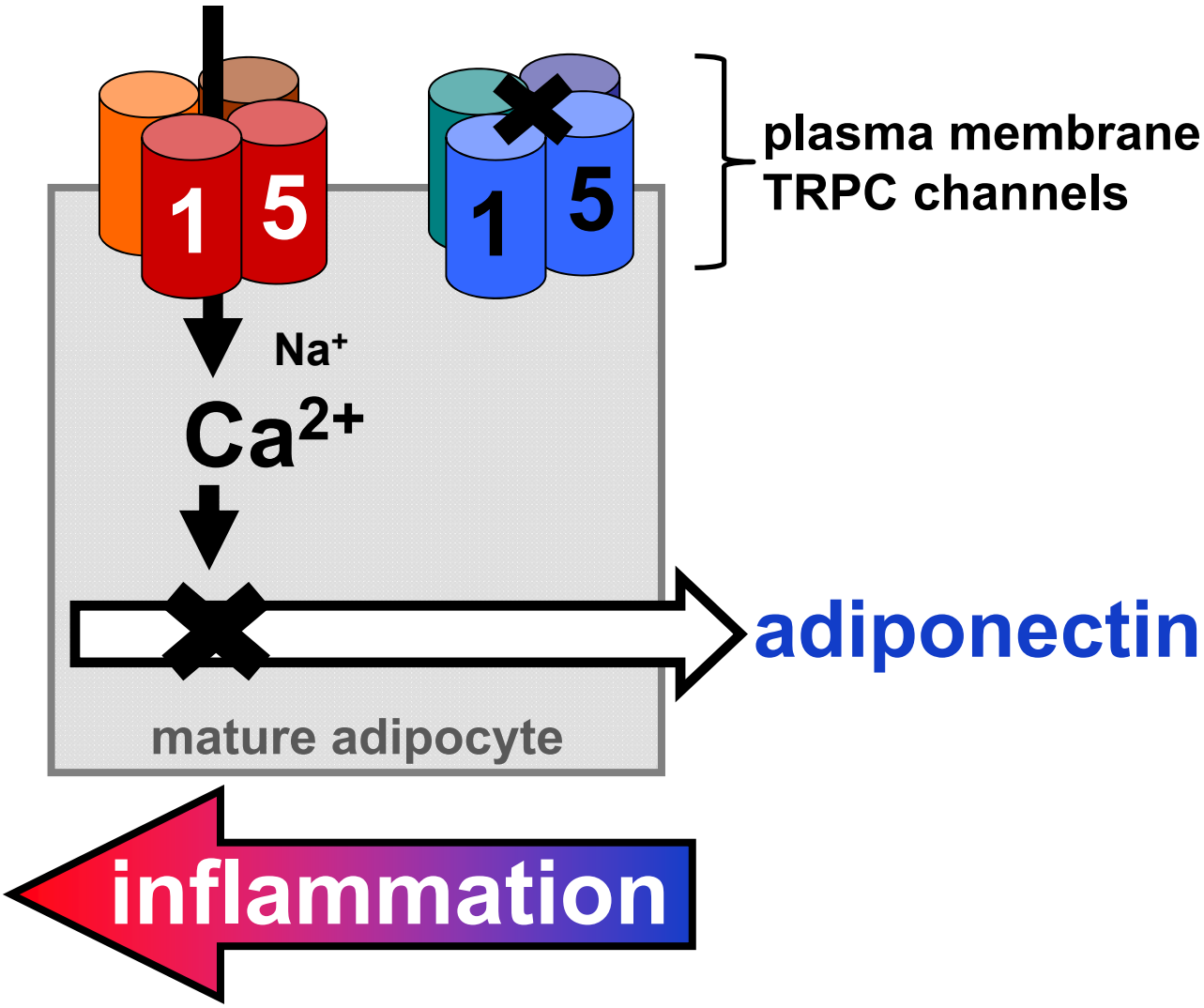

endothelial dysfunction
diabetes
hypertension
atherosclerosis
heart failure

Online Figure IX

Short-interfering (si) RNA molecules

Gene	siRNA
mTRPC1	GUUUCGUCUUGAUAUCUAU
mTRPC5	GCCUUGGGUUCUAGGUUUC

Online Table I

PCR primers

Target	Forward primer (5'-3')	Reverse Primer (5'-3')
Mouse PPARγ	ATTGAGTGCCGAGTCT	CTTCTGAAACCGACAGT
Mouse aP2	ATCAGCGTAAATGGGGA	CTCGTTTTCTCTTTATTGTGGTC
Mouse 18S	GATGCTCTTAGCTGAGTGT	GCTCTGGTCCGTCTTG
Mouse adiponectin	GTATCGCTCAGCGTTC	CGTTGACGTTATCTGCAT
Mouse Leptin	CATTTCACACACGCAGT	GGAGGTCTCGGAGATTC
Mouse TRPC1	AGCATCGTATTTCACATTCT	AGCCACCACTTTGAGG
Mouse TRPC3	GGCCTTCATGTTCGGT	AGGTTCTCCTTCTTCAGC
Mouse TRPC4	TGCTTCACGCCATCAG	GGGTCTTCGCTTGACA
Mouse TRPC5	TCGATATGAAGTGCTTGACC	CTCGACGACTCGGATT
Mouse TRPC6	TGAGAAAGAGTTCAAGAATGAC	GCTGCCGTAAACCAGA
Mouse TRPC7	CGAGACACAGAAGAGGT	GTTGCCGTAAGCCTGA
Mouse TRPV4	CACTGCGGACCTAGAT	CTGGCCTCGGTAGTAGA
Mouse TRPP2	GGTCTCTGGGGAACAAG	GGTGTCTATGAATAGCTGTG
Human TRPC1	GCTCTATCTTGGGTCCAT	GGCAGCACATCACTTT
Human TRPC5	ACATTTTAAGTTCGTTGCG	ACATCGGATCCCCTTG
Wild-type (WT) TRPC5	TTCGTTGCGTCTCATATCCC	TTCTCCGTCTACCGTCAGGG
Dominant negative (DN) TRPC5	CTCTTCAGTCAGCTGCAGCG	TTCTCCGTCTACCGTCAGGG
Mouse interleukin-6 (IL-6)	TGATGCACTTGCAGAAAACA	ACCAGAGGAAATTTTCAATAGGC
Mouse tumour necrosis factor α (TNFα)	CCACCACGCTCTTCTGTCTAC	AGGGTCTGGGCCATAGAACT

Online Table II

Fatty acids that inhibited TRPC5

Fatty acid	% inhibition
9(E)-octadecenoic acid	9.0 ± 2.6
8(Z),11(Z),14(Z)-eicosatrienoic acid	31.1 ± 0.7
7(Z),10(Z),13(Z),16(Z)-ocosatetraenoic acid	24.9 ± 2.7
undecanoic acid	38.3 ± 10.0
10(E)-pentadecenoic acid	8.3 ± 2.4
10(Z),13(Z)-nonadecadienoic acid	16.5 ± 0.2
5(Z),8(Z),11(Z),14(Z)-eicosatetraenoic acid	23.9 ± 4.5
9(Z),12(Z),15(Z)-octadecatrienoic acid (α-linolenic acid) (lino.)	23.4 ± 5.6
9(Z)-hexadecenoic acid	25.1 ± 5.5
9(Z),11(Z)-octadecadienoic acid	22.8 ± 4.6
11-dodecenoic acid	15.8 ± 4.6
9(E)-hexadecenoic acid	11.6 ± 3.9
14(Z)-tricosenoic acid	7.2 ± 2.6
4(Z),7(Z),10(Z),13(Z),16(Z),19(Z)-docosahexaenoic acid (DHA)	20.9 ± 6.0
12-tridecenoic acid	9.4 ± 2.7
10(E)-heptadecenoic acid	7.5 ± 1.9
6(Z),9(Z),12(Z)-octadecatrienoic acid	28.0 ± 9.2
9(Z)-tetradecenoic acid	40.6 ± 5.0
9(E)-tetradecenoic acid	16.7 ± 5.7

Online Table III

Fatty acids that had no effect on TRPC5

Decanoic acid	12(Z),15(Z)-Heneicosadienoic acid
10(Z)-Pentadecenoic acid	Tetracosanoic acid
10(E)-Nonadecenoic acid	5(Z)-Eicosenoic acid
11(Z)-Octadecenoic acid	Docosanoic acid
11(Z),14(Z),17(Z)-Eicosatrienoic acid	15(Z)-Tetracosenoic acid
Docosapentaenoic acid	Tetradecanoic acid
10-Undecenoic acid	Octadecanoic acid
Hexadecanoic acid	Nonadecanoic acid
11(E)-Octadecenoic acid	5(Z), 8(Z)-Eicosadienoic acid
Dodecanoic acid	13(Z)-Docosenoic acid
13(Z),16(Z),19(Z)-Docosatrienoic acid	6(Z)-Octadecenoic acid
Tricosanoic acid	7(Z)-Nonadecenoic acid
9(E),11(Z)-Octadecadienoic acid	7(Z),7(Z)-Dimethyleicosadienoic acid
11(E)-Eicosenoic acid	13(E)-Docosenoic acid
Heneicosanoic acid	6(E)-Octadecenoic acid
Tridecanoic acid	7(E)-Nonadecenoic acid
Heptadecanoic acid	11(Z),14(Z)-Eicosadienoic acid
9(E),12(E)-Octadecadienoic acid	13(Z),16(Z)-Docosadienoic acid
8(Z)-Eicosenoic acid	Pentadecanoic acid
12(Z) Heneicosenoic acid	9(Z)-Octadecenoic acid
14(E)-Tricosenoic acid	10(Z)-Nonadecenoic acid
12-Methoxydodecanoic acid	5(Z),8(Z),11(Z)-Eicosatrienoic acid
10(Z)-Heptadecenoic acid	
11(Z)-Eicosenoic acid	
Eicosanoic acid	

Online Table IV